Published in final edited form as:
J Cereb Blood Flow Metab. 2009 August ; 29(8): 1373–1382. doi:10.1038/jcbfm.2009.68.

MRI-based Characterization of Vascular Disruption by 5,6-dimethylxanthenone-acetic acid in Gliomas

Mukund Seshadri[1,2] and **Michael J Ciesielski**[3]

[1] Department of Cancer Biology, Roswell Park Cancer Institute, Buffalo, New York 14263, USA

[2] Preclinical Imaging Facility, Roswell Park Cancer Institute, Buffalo, New York 14263, USA

[3] Department of Neurosurgery, Roswell Park Cancer Institute, Buffalo, New York 14263, USA

Abstract

The well-vascularized nature of gliomas has generated a lot of interest in antiangiogenic therapies. However, the potential of vascular disrupting agents (VDAs) against gliomas has not been extensively investigated. In this study, we examined the *in vivo* efficacy of the tumor-VDA 5,6-dimethylxanthenone-4-acetic acid (DMXAA) against gliomas. Contrast-enhanced magnetic resonance imaging (MRI) and diffusion-weighted MRI were utilized to characterize the vascular and cellular response of GL261 and U87 gliomas to DMXAA treatment. Therapeutic efficacy was assessed by Kaplan-Meier survival analysis. Prior to VDA treatment, minimal enhancement was detected within the tumor in both models. Longitudinal relaxation rate ($R_1 = 1/T_1$) maps acquired 24 hours after treatment showed marked extravasation and accumulation of the contrast agent in the tumor indicative of treatment-induced vascular disruption. Normalized ΔR_1 values of the tumor showed a significant increase ($p<0.01$ GL261; $p<0.05$ U87) post therapy compared to baseline estimates. Mean apparent diffusion coefficient (ADC) values were significantly increased ($p=0.015$) 72 hours after therapy in GL261 but not in U87 gliomas. VDA therapy resulted in a significant ($p<0.01$) increase in median survival in both models evaluated. The results highlight the potential of VDAs against gliomas and the utility of MRI in the assessment of glioma response to VDA therapy.

Keywords

DMXAA; gliomas; MRI; VDAs

INTRODUCTION

Vascular proliferation is a critical component of glioma biology that strongly influences disease aggressiveness and patient survival (Brem, 1976; Abdulrauf *et al*, 1998; Cao *et al*, 2006). As a result, there has been considerable interest in therapies targeted towards tumor angiogenesis (Chamberlain, 2008). Several preclinical studies have reported the activity of antiangiogenic agents against gliomas (Sandstrom *et al*, 2004; Claes *et al*, 2008; Mathieu *et al*, 2008). Recent clinical studies have also investigated the activity of antiangiogenic agents in combination with chemotherapy with encouraging results (Narayana *et al*, 2009; Zuniga *et al*, 2009). Antiangiogenic agents such as bevacizumab are aimed at inhibiting new vessel formation by targeting specific angiogenic mediators or their receptors (Gerstner *et al*, 2007); in contrast, tumor-vascular disrupting agents (tumor-VDAs) such as combretastatin and 5,6-

Address correspondence and reprint requests to: Dr. Mukund Seshadri, Department of Cancer Biology, Cancer Cell Center - 164, Roswell Park Cancer Institute, Elm and Carlton Streets Buffalo, New York 14263, Ph: 716-845-1552, Fax: 716-845-1764, Mukund.Seshadri@roswellpark.org.

dimethylxanthenone-4-acetic acid (DMXAA) lead to disruption of existing tumor vasculature (Tozer *et al*, 2005). Although the activity of VDAs against a variety of tumor types has been reported in preclinical model systems, only a few studies have examined the potential of VDA therapy against gliomas. Published reports of studies investigating the activity of VDAs against gliomas have also been carried out only in ectopic (subcutaneous) brain tumors (Eikesdal *et al*, 2002; Wachsberger *et al*, 2005). Since tumor vascularization is an important characteristic of glioma biology, we hypothesized that selective disruption of tumor vasculature could be of potential therapeutic benefit in gliomas. To test this hypothesis, we examined the therapeutic activity of the small molecule tumor-VDA DMXAA (Rehman and Rustin, 2008) against two experimental orthotopic models, murine GL261 gliomas and human U87 glioma xenografts. Using an imaging-based approach, we characterized the response of the two glioma models to DMXAA treatment.

Imaging techniques such as magnetic resonance imaging (MRI) and positron emission tomography (PET) constitute an integral component of the diagnostic and therapeutic assessment of gliomas (Gerstner *et al*, 2008; Sorensen *et al*, 2008). Among the radiologic techniques currently available, MRI offers several advantages including excellent soft tissue contrast, high temporal and spatial resolution without the use of ionizing radiation or radioactive tracers. Specifically, contrast-enhanced MRI (CE-MRI), a technique that provides information pertaining to tumor vascular physiology, is widely being used to evaluate the biological activity of targeted therapies in preclinical models and in clinical trials (Akella *et al*, 2004; Jackson *et al*, 2007). In neuro-oncology, CE-MRI has been used to estimate parameters such as cerebral blood volume and vascular permeability in gliomas (Cao *et al*, 2006; Claes *et al*, 2008; Akella *et al*, 2004). Therefore, in this study, using CE-MRI, we prospectively investigated the early vascular changes in murine GL261 gliomas and human U87 glioma xenografts following treatment with the tumor-VDA DMXAA. The study included a baseline CE-MRI examination prior to DMXAA treatment and a follow up study at 24 hours post treatment.

Another MRI technique that is being widely investigated in preclinical and clinical studies for its utility as a biomarker of therapeutic response is diffusion-weighted MRI (DW-MRI) (Hamstra *et al*, 2008). DW-MRI is a sensitive technique that allows detection of early cellular changes in tumors based on the Brownian motion of water (Koh *et al*, 2007). In experimental animal models, DW-MRI has been shown to provide tumor-specific information that strongly correlates with treatment response (Lee *et al*, 2006). Measurement of the apparent diffusion coefficient (ADC) from DW-MRI data sets has been correlated with disease progression and survival in patients with brain tumors (Hamstra *et al*, 2008). Therefore, in addition to CE-MRI, DW-MRI was performed 72 hours post treatment and apparent diffusion coefficient (ADC) maps calculated to examine changes in water mobility as a measure of tumor response to DMXAA.

Finally, to determine the long-term therapeutic efficacy of DMXAA against the two glioma models, animals were monitored over a 40-day period and differences in survival between control and treatment groups were assessed by Kaplan-Meier analysis. The results of our studies demonstrate for the first time potent tumor vascular disruption following DMXAA treatment in both glioma models evaluated. A statistically significant increase in median survival was also observed following VDA treatment compared to untreated controls.

MATERIALS AND METHODS

Cell lines and culture conditions

GL261 murine glioma cells and U87 human glioma cells were grown on 100-mm tissue culture plates in complete Dulbecco's modified Eagle's medium (DMEM) containing 10% fetal calf

serum, 5,000 units penicillin/streptomycin at 37°C in 5% CO_2 with media changes two to three times per week.

Tumor models

C57Bl6 mice and athymic NCr-nu/nu nude mice were purchased from the National Cancer Institute, Rockville, MD for establishing GL261 and U87 gliomas, respectively. Animals were provided food and water *ad libitum* and housed in micro isolator cages in a laminar flow unit under ambient light. The procedure for intracerebral implantation of tumor cells has been previously described (Ciesielski *et al*, 2006).Briefly, eight-to-twelve week old mice were anesthetized by intraperitoneal (i.p.) injection of ketamine:xylazine anesthetic cocktail and fixed in a stereotactic head frame (David Kopf Instruments, Tujunga, CA). A midline scalp incision was made and the bregma was identified. Stereotactic coordinates were measured (2.0 mm lateral, and 1.0 mm anterior to the bregma) for implantation of cells into the deep frontal white matter. A burr hole was drilled at this point and 1×10^5 GL261 cells or 5×10^5 U87 cells suspended in 5 μl of DMEM were injected through a Hamilton syringe with a fixed, 25-gauge needle at a depth of 3.0 mm relative to the dura mater. Injections were performed at 1μl/min. Following implantation of tumor cells, the needle was slowly withdrawn, the incision sutured and the animal monitored for recovery. All experimental studies were performed in accordance with protocols approved by the Institutional Animal Care and Use Committee (IACUC) at Roswell Park Cancer Institute.

Experimental Design

The basic study design for investigating the antivascular and antitumor activity of DMXAA against gliomas is shown schematically in Figure 1A. Approximately 3 weeks post implantation, high-resolution T2-weighted (T2W) MR images were acquired to confirm presence of tumor growth. Contrast-enhanced MRI examinations were performed using T_1-weighted fast spin-echo images over a two-day period as described below. Following baseline image acquisition, DMXAA powder was dissolved in phosphate buffered saline or D5Wsolution prior to administration. C57Bl6 mice bearing GL261 gliomas were treated with a single dose of DMXAA (30 mg/kg, i.p.). Although this is the documented maximum tolerated dose (MTD) of DMXAA in mice, we have observed that some strains of nude and severe combined immunodeficiency (SCID) mice do not tolerate this dose. Therefore, based on preliminary toxicity studies carried out in the laboratory, nude mice bearing intracranial U87 gliomas were treated with a single dose of 27.5 mg/kg DMXAA (i.p.). Treatment was administered to mice used for imaging studies following baseline MRI acquisition and a second set of contrast-enhanced T_1W images were acquired 24 hours post treatment to visualize glioma vascular response to treatment. Additionally, DW-MRI was performed 72 hours post treatment to detect intratumoral changes in cellularity following treatment. Treatment efficacy was assessed by monitoring survival of control and DMXAA-treated mice over a 40-day period.

Magnetic resonance imaging

Experimental imaging studies were carried out in a 4.7T/33-cm horizontal bore magnet (GE NMR Instruments, Fremont, CA) incorporating AVANCE digital electronics (Bruker Biospec, ParaVision 3.1., Bruker Medical, Billerica, MA), a removable gradient coil insert (G060, Bruker Medical) generating a maximum field strength of 950 mT/m, and a custom designed 35 mm radiofrequency transmit/receive coil. Anesthesia was induced prior to image acquisition using 3–3.5% Isoflurane (Abbott Laboratories, IL) and maintained at ~2–2.5% during image acquisition. Animals were secured in a form-fitted MR-compatible mouse sled equipped with temperature and respiratory sensors (Dazai Research Instruments, Toronto, Canada). An air heater system (SA Instruments Inc., Stony Brook, NY, Model 1025) was used to maintain animal body temperature during image acquisition. A thermocouple embedded within the sled

provided automated temperature control feedback. Care was taken to maintain animal body temperature and minimize motion during image acquisition.

The first set of MRI examinations was performed 8–10 days after intracerebral inoculation of tumor cells to confirm successful growth of tumors. Preliminary localizer images were acquired in the sagittal and axial planes prior to acquisition of T_1 and T_2-weighted scans. T_2-weighted fast spin-echo (SE) images were acquired on coronal and axial planes to determine the presence and extent of tumors using the following parameters: TE_{eff} = 75 ms, TR = 3370 ms, echo train length = 8, field of view (FOV) = 32mm, matrix size = 256 × 256, 1mm thick slices, number of averages = 4, acquisition time = 7m29s. CE-MRI was performed using the intravascular contrast agent albumin-gadopentetate dimeglumine [albumin-$(Gd\text{-}DTPA)_{35}$] according to methods previously described by us (Seshadri *et al*, 2006). At least 2–3 slices of the tumor were positioned for T_1 measurements using the T_2-weighted coronal images as reference. Multislice relaxation rate ($R_1 = 1/T_1$) maps were obtained using a saturation recovery, fast spin echo (FSE) scan with variable repetition times (TR). The scan parameters were as follows: slice thickness = 1mm, TE_{eff} = 25 ms, 128 × 96 matrix, 32 mm FOV, echo train length = 4, TR = 360–6000 ms, acquisition time = 4m50s. Three precontrast T1-weighted FSE images were acquired to obtain an average estimate of precontrast T1-values. Albumin-$(Gd\text{-}DTPA)_{35}$ (*courtesy of* Dr. Robert Brasch, University of California – San Francisco) was then administrated at a dose of 0.1 mmol/kg as a bolus *via* tail-vein injection and a second set of seven T1-weighted FSE images were acquired. Since each individual FSE scan was ~5 minutes in duration, this allowed for estimation of R1 for ~45 minutes post contrast agent administration. The T_1-relaxivity of the agent as determined at the Center for Pharmaceutical and Molecular Imaging, Department of Radiology, University of California San Francisco (UCSF) was 11.0 $(mM{\cdot}s)^{-1}$ per Gd ion, at 25°C and 10 MHz.

DW-MRI was performed using a multislice diffusion-weighted spin echo sequence with the following acquisition parameters: TE/TR = 30/1200 ms, 128 × 128 matrix, 3.2 × 3.2 cm, diffusion gradient strength (four variable gradient strengths per acquisition) = 8, 128, 256, 420 mT/m; diffusion B value (corresponding to four variable B values per acquisition) = 2.9, 512, 2036.3; 5470 s/mm^2; diffusion gradient duration = 6 ms; diffusion gradients applied in X, Y and Z directions; number of averages = 2, 1 mm slice thickness with a total data acquisition time of 20m28s. Measurements were obtained at baseline (prior to DMXAA administration) and 72 hours post treatment.

Image processing and analysis

Following image acquisition, raw image sets were transferred to a processing workstation and converted into Analyze™ format (AnalyzeDirect, Version 8.0, Overland Park, KS). Raw data was reformatted and object maps of regions-of-interest (ROI) - tumor, muscle, contra lateral brain tissue and background noise were manually traced.

The relaxation rate R_1 ($R_1 = 1/T_1$) and the maximal signal intensity S_{max} were calculated following subtraction of background noise using the following equation

$$S_{TR} = S_{max}(1 - e^{-(R1 * TR)})$$

where S_{TR} is the signal intensity obtained at each TR time. R_1 values obtained from the three precontrast scans and the seven post contrast scans were averaged for tumor, brain and muscle tissues and the difference between the two values reported as normalized ΔR_1 (tumor/muscle). The change in relaxation rate (ΔR_1) following contrast agent administration was assumed to be proportional to the concentration of the agent in tissue. R_1 maps were calculated on a pixel-

by-pixel basis using MATLAB (Version 7.0, Mathworks Inc., Natick, MA). A low-pass filter and a pseudo-color scale were applied in Analyze™ for visualization.

ADC values were computed on a pixel-by-pixel basis by fitting the images from the DW-MRI sequence to the following equation

$$M_b = M_0 e^{(-(ADC)*B}$$

where M_b and M_0 are the MR signal intensities with and without diffusive attenuation, respectively, and B is the diffusion weighting factor. ADC maps were generated by fitting the raw data to the above equation using non-linear regression analysis in MATLAB.

Survival analysis

Animals were observed for clinical symptoms including weight loss (>20%), loss of movement, seizures and ataxia and euthanized according to institutional guidelines. The log-rank test was used to analyze statistical differences between Kaplan-Meier survival curves of animals in the control and treatment groups over a 40-day period.

Statistical considerations

All statistical analyses were performed using GraphPad Prism version 5.00 for Windows (GraphPad Software, San Diego California USA, www.graphpad.com). Measured values are reported as the mean ± standard error of the mean. The two-tailed *t*-test was used for comparing CE-MRI data at baseline and post treatment time points and *p*-values <0.05 were considered statistically significant. In total, 18 C57Bl6 mice (12 controls, 6 treated) and 23 nude mice (13 controls, 10 treated) were used for experimental studies. CE-MRI results presented represent paired data sets obtained at baseline and 24h post treatment time points for a total of 9 mice (4 C57Bl6 bearing GL261 gliomas and 5 *nu/nu* mice bearing U87 glioma xenografts). Reported results of DW-MRI represent paired observations obtained at baseline and 72 hours post treatment time points in 3 animals with GL261 gliomas. Paired two-tailed *t* test analysis with Bonferroni correction was utilized to examine differences between baseline and 72h post treatment ADC values for the whole tumor, contra lateral brain and muscle tissues.

RESULTS

T2-weighted MRI

To visualize glioma growth, T2-weighted (T2W) MR images were acquired at different times post intracranial implantation of tumor cells. Both GL261 and U87 gliomas appeared as well-defined hyper intense regions (*arrows*) at the site of injection on non contrast-enhanced T2W spin-echo images (Figure 1B). The presence of tumor was confirmed using T2W MRI on all the animals used for therapeutic evaluation.

T1-weighted CE-MRI

Vascular response of Gl261 and U87 tumors to DMXAA treatment was evaluated using CE-MRI with albumin-$(GdDTPA)_{35}$, a well characterized intravascular MR contrast agent that has been extensively used in preclinical studies (Schmiedl *et al*, 1990). The study included a baseline MR examination prior to DMXAA treatment and a follow up study at 24 hours post treatment. R_1 maps ($R_1 = 1/T_1$) were calculated on a pixel-by-pixel basis before and after DMXAA treatment to visualize treatment-induced changes in vascular integrity. Figure 2A shows colorized post contrast R1maps of a C57Bl6 mouse brain bearing an intracranial GL261 glioma before (*pretreatment*) and 24 hours after DMXAA treatment (24h post). Corresponding

T_2W images of the brain depicting the location of the tumor (*arrows*) are also shown. Minimal tumor enhancement was seen following administration of the contrast agent (postcontrast 1) with no visible increase over the 45 minute post contrast imaging period (post contrast 7) prior to DMXAA treatment (*pretreatment*). In sharp contrast, 24 hours post treatment, marked extravasation and accumulation of the contrast agent was visible on the post contrast R_1 maps of the same animal indicative of significant vascular disruption following treatment (*24h post*). The longitudinal relaxation rate ($R_1 = 1/T_1$) of tissues is linearly related to contrast agent concentration. Therefore, the mean ΔR_1 values of the tumor were calculated and normalized to ΔR_1 muscle tissue to provide an indirect estimate of intratumoral contrast agent concentration at baseline and post treatment time points. As shown in Figure 2B, a near 5-fold increase ($p<0.001$, n=4) in normalized ΔR_1 tumor/muscle value (1.7 ± 0.26) was observed at 24 hours post treatment compared to baseline estimates (0.36 ± 0.05) indicative of DMXAA-induced vascular disruption.

Using the same study design, the vascular response of U87 gliomas was investigated. Baseline and post treatment R_1 maps (first and last post contrast scans) of a nude mouse bearing a U87 glioma are shown in Figure 3A. Similar to GL261 tumors, minimal tumor enhancement was seen at baseline. Twenty four hours after treatment, evidence of vascular disruption in the form of increased contrast agent accumulation within the tumor was observed on postcontrast R_1maps (Figure 3A). However, visible changes in R1 maps were much less pronounced in U87 xenografts compared to GL261 tumors. Normalized $\Delta R_{1\text{tumor/muscle}}$ values of U87 gliomas (Figure 3B) also showed only a minimal increase in contrast agent concentration at the 24 hour time point (0.85 ± 0.04) compared to baseline estimates (0.65 ± 0.07, $p<0.05$, n=5).

Diffusion-weighted MRI

DW-MRI was performed 72 hours post treatment and apparent diffusion coefficient (ADC) maps were calculated to examine changes in water mobility as a measure of tumor response to DMXAA. Figure 4A shows pseudo-colorized ADC maps of a GL261 glioma overlaid on the corresponding T_2W images of a C57Bl6 mouse prior to and 72 hours post therapy. Enlarged views of the tumor (ROI) are also shown. Regions of higher ADC were observed in GL261 gliomas at the 72 hour time point compared to baseline measurement indicative of a response. ADC values of all 3 animals scanned at the 72 hour post treatment time point showed an increase compared to baseline estimates (Figure 4B). The mean ADC values of all 3 animals at baseline was calculated to be 0.67 ± 0.06 (1 $x10^{-3}mm^2/s$. Seventy-two hours post treatment, an ~13% increase in mean ADC values (0.75 ± 0.05, $p=0.015$) was observed in GL261 gliomas. DW-MRI of nude mice bearing U87 gliomas revealed no significant difference in ADC values (*data not shown*) 72h post DMXAA treatment (n=3) compared to baseline values or untreated controls (n=4). Statistical analysis of ADC values of contralateral normal brain tissue did not show any difference between the two time points.

Long-term efficacy of VDA therapy

We then examined the long-term consequence of tumor vascular disruption induced by DMXAA in both glioma models by monitoring long-term survival following treatment. Median survival of control and DMXAA-treated animals was calculated using the method of Kaplan and Meier and differences analyzed for statistical significance using the log rank test. As shown in Figure 5, a significant but differential increase in median survival was observed following DMXAA treatment in GL261 and U87 models. The median overall survival of control C57Bl6 (n=12) mice bearing GL261 gliomas was 19.5 days (Figure 5A). In comparison, GL261 tumor-bearing animals treated with DMXAA (n=6) showed a median survival 29 days ($p=0.003$, log-rank test). In the U87 xenograft model, DMXAA treated animals (n=10) exhibited a median survival of 34-days ($p=0.0005$, log-rank test) compared to untreated control animals (n=13) that exhibited a median survival of 26 days from the day of

implantation (Figure 5B). Overall, animals treated with DMXAA exhibited significantly prolonged survival (~50% for GL261 and ~30% for U87 gliomas) compared to untreated controls.

DISCUSSION

The aggressive clinical course of gliomas often limits treatment options and contributes to poor long-term survival in patients. The need to investigate and develop novel and effective therapies in gliomas is therefore clearly evident.

The molecular and phenotypic differences between normal tissue vasculature and tumor-associated vasculature offer a unique opportunity that has been exploited for selective therapeutic targeting (Eberhard et al., 2000; Ruoslahti, 2002). This has been pursued primarily using two approaches: (i) antiangiogenic agents such as bevacizumab and DC101 that are aimed at preventing or inhibiting new vessel formation typically by targeting a specific angiogenic molecule or its membrane receptor (Jain, 2001; Tong *et al*, 2004), and (ii) vascular disrupting agents (VDAs) that selectively destroy existing tumor vessels (Kelland, 2005). Examples of VDAs include combretastatin, ZD6126 and the small molecule DMXAA (ASA404). It is believed that VDAs differ from antiangiogenic agents both in their mode of action and in their potential clinical application. VDAs are targeted towards larger solid tumors with established vasculature in contrast to antiangiogenic agents targeted towards smaller tumors with associated neovasculature (Kelland, 2005).

Gliomas are highly angiogenic, aggressive brain tumors that are often non-responsive to therapy (Brem, 1976; Abdulrauf *et al*, 1998; Cao *et al*, 2006). Changes associated with angiogenesis in gliomas have been correlated with an aggressive disease phenotype and poor clinical outcome (Abdulrauf *et al*, 1998; Cao *et al*, 2006). These observations have led to the investigation of the potential of antiangiogenic agents in gliomas in preclinical and clinical settings (Claes et al, 2008; Narayana *et al*, 2009). However, the potential of VDAs against gliomas has not been extensively reported. Therefore, in this study, we investigated the antivascular activity and efficacy of the tumor-VDA DMXAA against gliomas. The agent has been shown to be well-tolerated in Phase I clinical trials (McKeage *et al*, 2006). Results of a randomized Phase II clinical trial in patients with non-small cell lung cancer has also demonstrated improvement efficacy with DMXAA in combination with carboplatin and paclitaxel (McKeage *et al*, 2008). Using MRI, we examined the response of intracranial GL261 murine gliomas and U87 human glioma xenografts to VDA therapy along with long-term survival analysis. Our results demonstrate potent antivascular activity of DMXAA that translated into a survival benefit in both models evaluated.

Radiologic techniques are important components of the diagnostic and prognostic armamentarium in neuro-oncology (Gerstner *et al*, 2008). A number of non-invasive imaging methods including PET, perfusion computed tomography (CT) and MRI are currently being used to evaluate the activity of targeted therapies in clinical trials. Contrast-enhancement within tissue detected by MRI or CT is commonly used as an indicator of malignant progression in gliomas (Gerstner *et al*, 2008; Sorensen *et al*, 2008). Clinical trials of antiangiogenic agents have utilized CE-MRI for the assessment of biological activity with encouraging results (Akella *et al*, 2004). Most CE-MRI studies are typically performed using a paramagnetic contrast agent that results in the shortening of the longitudinal (T_1) relaxation time of tissues. Tissue blood volume is extracted from changes in signal intensity through the application of a pharmacokinetic model with associated assumptions. However, the use of freely diffusible tracers has led to difficulties in interpretation, particularly following treatment with antiangiogenic agents.

The amount and rate of contrast agent uptake within a tissue following intravenous administration is related to the extent of tissue blood supply (perfusion) and transendothelial transport (diffusion) of the agent. With small molecular weight agents that freely diffuse across the endothelium, the intravascular concentration of the contrast agent following administration of a bolus injection decreases with time during the course of a single MR examination. Since large molecular weight contrast agents exhibit minimal transendothelial diffusion and remain intravascular for longer periods of time, these agents are considered to be more suited as probes for assessing tumor vascular permeability compared to small molecular weight agents (Brasch *et al*, 1997; Barrett *et al*, 2006). Therefore, in this study, CE-MRI was performed with an intravascular contrast agent to characterize the vascular response of gliomas to VDA therapy. The agent used in our study has been well-characterized and widely used in preclinical studies to estimate tumor vascular permeability (Schmiedl *et al*, 1990; Raatschen *et al*, 2008). Since the relaxation rate of tissues and not signal intensity is linearly related to contrast agent concentration, the change in tissue longitudinal relaxationrate (ΔR_1) following intravenous administration of the contrast agent was used as an indirect estimate of its tissue concentration. Dynamic R_1 mapping was used to visualize the effect of VDA therapy on glioma vasculature.

Antiangiogenic agents have been shown to decrease tumor vascular permeability and interstitial fluid pressure while inhibiting new vessel formation (Tong *et al*, 2004). These 'normalizing' effects are believed to contribute to a functionally efficient vascular network thereby improving drug delivery and penetration (Jain, 2001). In contrast, VDAs such as combretastatin-A4-phosphate and DMXAA affect the structure and integrity of the tumor endothelial lining resulting in alterations in vascular permeability, eventually leading to blood flow stasis and shutdown (Tozer *et al*, 2005; Kelland, 2005). Previous reports by us and others have demonstrated increased vascular permeability as the major mechanism of action of the VDA DMXAA (Zhao *et al*, 2005; Seshadri *et al*, 2005). Consistent with these known, previously observed biological effects of VDAs, the results of our CE-MRI studies provided evidence of marked alterations in vascular permeability in both models 24 hours following treatment (Figures 2 and 3). Treatment with DMXAA led to considerable extravasation of the contrast agent as demonstrated by the significant increase in R1 post treatment compared to baseline levels.

In addition to CE-MRI, we utilized DW-MRI to assess changes in cellularity of gliomas following treatment. The technique is widely being investigated in preclinical and clinical systems for its utility as a biomarker of disease and therapeutic response (Lee *et al*, 2006; Hamstra *et al*, 2008). The principles and the biological basis of DW-MRI has been extensively described (Koh *et al*, 2007; Hamstra *et al*, 2008). The technique measures the random brownian motion of water molecules within biological tissues (free diffusion) as an indirect measure of tissue cellularity and membrane integrity (Hamstra *et al*, 2008). In DW-MRI, a quantitative estimate of the mobility of water protons is obtained by calculation of the ADC from the detected attenuation in signal intensity within tissue (Koh *et al*, 2000; Lee *et al*, 2006). Parametric mapping of ADC values provides a visual estimate of changes in cellularity within a given tissue of interest. Highly cellular regions in tissue with restricted water diffusion are associated with low ADC values and correspondingly, regions with low cellularity exhibit higher ADC values (Lee *et al*, 2006; Hamstra *et al*, 2008; Koh *et al*, 2007).

In the present study, DW-MRI revealed a significant increase in mean ADC values of GL261 gliomas 72 hours post treatment compared to baseline estimates (Figure 4). ADC maps revealed a heterogeneous pattern of response to DMXAA at the 72 hour time point. This could be reflective of the spatial variation in tumor vascular damage-induced by DMXAA since VDAs are believed to be more effective in the central regions of the tumor containing established vasculature (Tozer *et al*, 2005). The classical pattern of tumor response to VDAs reported in preclinical studies involves induction of central necrosis with a fraction of viable cells found

in the periphery that survive treatment (Tozer *et al*, 2005). While spatial correlation between the vascular damage (R1 change) and cell death (ADC change) would have yielded useful results, this was not performed due to the difference in time points between CE-MRI and ADC data acquisitions.

Consistent with the less pronounced vascular response observed with CE-MRI, DW-MRI of U87 xenografts did not reveal a significant change in ADC following treatment. This is not surprising when considering the difference in DMXAA dose used between the two models. DMXAA has been observed to exhibit a rather steep dose-response curve in preclinical model systems with significant species and strain differences in pharmacokinetics. Since the aim of our study was to evaluate the response of murine gliomas and human glioma xenografts to DMXAA rather than to compare differences in their response, we utilized two different but well-tolerated doses of DMXAA (30 mg/kg for GL261 tumors and 27.5 mg/kg for U87 tumors). This could at least partly explain the differences in degree of response between the two models as detected by DW-MRI and the survival benefit observed (10 days for GL261; 8 days for U87). Additionally, the vascular disruptive effects of DMXAA are a consequence of both direct drug effects on the endothelium and indirect effects through induction of cytokines such as tumor necrosis factor-alpha (Baguley and Wilson, 2002). In a recent study, we have demonstrated differences in cytokine induction and the vascular response of ectopic and orthotopic murine fibrosarcomas established in C57Bl6 mice treated with the same dose of DMXAA (Seshadri *et al*. 2008). It is therefore plausible that variable degrees of cytokine induction between GL261 and U87 gliomas following DMXAA treatment could have also contributed to the observed differences in vascular response and survival. However, given differences in the underlying tumor biology (disease aggression, angiogenic characteristics) between the two models, it is difficult to make valid conclusions on the differential response observed between U87 and GL261 models. One potential alternative that could be considered for future studies would be to examine the possibility of implanting GL261 tumors in nude mice. Such a design would eliminate one variable (mouse strain) and enable utilization of the same dose of the agent against both tumors.

Finally, a discussion of the implications and the limitations of the study is warranted. Although only a single dose of DMXAA was evaluated, treatment with a single injection of the tumor-VDA resulted in a statistically significant survival benefit in both glioma models evaluated (Figure 5). However, we observed no evidence of ‘cure’ with VDA treatment. Given the data obtained from several preclinical reports (Baguley and Wilson, 2002) suggesting that the true value of VDAs lies in their use in combination with chemo- or radio-therapy, this is not an entirely surprising observation. Secondly, the blood brain barrier (BBB) is a critical factor that influences delivery of chemotherapeutic agents to brain tumors (Gerstner and Fine, 2007). Studies in preclinical models have shown that treatment with antiangiogenic agents reduces the permeability of BBB through stabilization of the vasculature (Claes *et al*, 2008;Mathieu *et al*, 2008). In contrast, treatment with hyper osmotic agents such as mannitol have also been shown to result in disruption of the BBB and contribute to enhanced efficacy of boron neutron capture therapy (Barth *et al*, 2000). In our study, contrast-enhanced MRI provided evidence of disruption of the BBB following VDA treatment in both glioma models. It could therefore be hypothesized that optimization of dose and schedule of VDAs such as DMXAA in combination with chemotherapy would potentially enable increased drug delivery to gliomas. We are currently planning to evaluate the combination of DMXAA with chemotherapeutic agents such as temozolomide against gliomas to test this hypothesis. And finally, there has been an increased interest in the identification of early biomarkers that can reliably predict disease aggression or therapeutic response. With the increased development of targeted therapies, it is believed that imaging methods are likely to provide indirect evidence of the early biological activity of these agents. Specific MRI parameters of tumor vascularity and cellularity are currently being investigated for their potential value in predicting tumor response

to conventional and novel anticancer therapies. In our study, CE-MRI allowed measurement of the early changes in vascular permeability following DMXAA treatment. This observation is particularly important since enhancement of vascular permeability is the major mechanism of action of the agent consistently observed in preclinical models (Zhou *et al*, 2005; Seshadri *et al*, 2005). Therefore, MRI measurements of permeability using an intravascular contrast agent could potentially serve as a surrogate marker of efficacy that is mechanistically related to pharmacologic activity of DMXAA. However, in our study, due to the relatively small sample size used in the imaging study, we did not perform direct correlation between the early vascular response and treatment outcome. Further examination with a larger cohort of animals is required to determine the true predictive ability of such MRI based biomarkers. Recent clinical approval of the intravascular MR contrast agent, MS-325 (Vasovist™) for MR angiography (MRA) at least offers the potential of incorporating the methodology for the assessment of biological activity of VDAs in patients in the future.

In conclusion, our findings demonstrate proof-of-principle of the potential of antivascular therapy in gliomas. To the best of our knowledge, this is the first report on the antivascular and antitumor activity of DMXAA in two orthotopic glioma models.

Acknowledgments

The authors would like to thank Drs. Robert Brasch and Yanjun Fu (University of California, San Francisco) for providing albumin-GdDTPA; Dr. Joseph Spernyak (RPCI) for useful discussions; Steve Turowski and Alison Arter for technical assistance.

Funding sources: This research was supported by the Roswell Park Alliance Foundation and Linda Scime Endowment Fund and utilized core resources supported by the Cancer Center Support Grant by the National Cancer Institute (CA-16056).

References

1. Abdulrauf SI, Edvardsen K, Ho KL, Yang XY, Rock JP, Rosenblum ML. Vascular endothelial growth factor expression and vascular density as prognostic markers of survival in patients with low-grade astrocytoma. J Neurosurg 1998;88:513–20. [PubMed: 9488306]
2. Akella NS, Twieg DB, Mikkelsen T, Hochberg FH, Grossman S, Cloud GA, Nabors LB. Assessment of brain tumor angiogenesis inhibitors using perfusion magnetic resonance imaging: quality and analysis results of a phase I trial. J Magn Reson Imaging 2004;20:913–22. [PubMed: 15558578]
3. Baguley BC, Wilson WR. Potential of DMXAA combination therapy for solid tumors. Expert Rev Anticancer Ther 2002;2:593–603. [PubMed: 12382527]
4. Barrett T, Kobayashi H, Brechbiel M, Choyke. Macromolecular MRI contrast agents for imaging tumor angiogenesis. Eur J Radiol 2006;60:353–66. [PubMed: 16930905]
5. Barth RF, Yang W, Rotaru JH, Moeschberger ML, Boesel CP, Soloway AH, Joel DD, Nawrocky MM, Ono K, Goodman JH. Boron neutron capture therapy of brain tumors: enhanced survival and cure following blood-brain barrier disruption and intracarotid injection of sodium borocaptate and borophenylalanine. Int J Radiat Oncol Biol Phys 2000;47:209–18. [PubMed: 10758326]
6. Brasch R, Pham C, Shames D, Roberts T, van Dijke K, van Bruggen N, Mann J, Ostrowitzki S, Melnyk O. Assessing tumor angiogenesis using macromolecular MR imaging contrast media. J Magn Reson Imaging 1997;7:68–74. [PubMed: 9039595]
7. Brem S. The role of vascular proliferation in the growth of brain tumors. Clin Neurosurg 1976;23:440–53. [PubMed: 975695]
8. Cao Y, Nagesh V, Hamstra D, Tsien CI, Ross BD, Chenevert TL, Junck L, Lawrence TS. The extent and severity of vascular leakage as evidence of tumor aggressiveness in high-grade gliomas. Cancer Res 2006;66:8912–7. [PubMed: 16951209]
9. Chamberlain MC. Antiangiogenic blockage: a new treatment for glioblastoma. Expert Opin Biol Ther 2008;8:1449–53. [PubMed: 18774913]

10. Ciesielski MJ, Apfel L, Barone TA, Castro CA, Weiss TC, Fenstermaker RA. Antitumor effects of a xenogeneic survivin bone marrow derived dendritic cell vaccine against murine GL261 gliomas. Cancer Immunol Immunother 2006;55:1491–503. [PubMed: 16485128]
11. Claes A, Gambarota G, Hamans B, van Tellingen O, Wesseling P, Maass C, Heerschap A, Leenders W. Magnetic resonance imaging-based detection of glial brain tumors in mice after antiangiogenic treatment. Int J Cancer 2008;122:1981–6. [PubMed: 18081012]
12. Eberhard A, Kahlert S, Goede V, Hemmerlein B, Plate KH, Augustin HG. Heterogeneity of angiogenesis and blood vessel maturation in human tumors: implications for antiangiogenic tumor therapies. Cancer Res 2000;60:1388–93. [PubMed: 10728704]
13. Eikesdal HP, Landuyt W, Dahl O. The influence of combretastatin A-4 and vinblastine on interstitial fluid pressure in BT4An rat gliomas. Cancer Lett 2002;178:209–17. [PubMed: 11867206]
14. Gerstner ER, Fine RL. Increased permeability of the blood-brain barrier to chemotherapy in metastatic brain tumors: establishing a treatment paradigm. J Clin Oncol 2007;25:2306–12. [PubMed: 17538177]
15. Gerstner ER, Duda DG, di Tomaso E, Sorensen G, Jain RK, Batchelor TT. Antiangiogenic agents for the treatment of glioblastoma. Expert Opin Investig Drugs 2007;16:1895–908.
16. Gerstner ER, Sorensen AG, Jain RK, Batchelor TT. Advances in neuroimaging techniques for the evaluation of tumor growth, vascular permeability, and angiogenesis in gliomas. Curr Opin Neurol 2008;21:728–35. [PubMed: 18989120]
17. Hamstra DA, Galbán CJ, Meyer CR, Johnson TD, Sundgren PC, Tsien C, Lawrence TS, Junck L, Ross DJ, Rehemtulla A, Ross BD, Chenevert TL. Functional diffusion map as an early imaging biomarker for high-grade glioma: correlation with conventional radiologic response and overall survival. J Clin Oncol 2008;26:3387–94. [PubMed: 18541899]
18. Jackson A, O'Connor JP, Parker GJ, Jayson GC. Imaging tumor vascular heterogeneity and angiogenesis using dynamic contrast-enhanced magnetic resonance imaging. Clin Cancer Res 2007;13:3449–59. [PubMed: 17575207]
19. Jain RK. Normalizing tumor vasculature with anti-angiogenic therapy: a new paradigm for combination therapy. Nature Med 2001;7:987–9. [PubMed: 11533692]
20. Kelland LR. Targeting established tumor vasculature: A novel approach to cancer treatment. Curr Cancer Ther Rev 2005;1:1–9.
21. Koh DM, Collins DJ. Diffusion-weighted MRI in the body: applications and challenges in oncology. AJR Am J Roentgenol 2007;188:1622–35. [PubMed: 17515386]
22. Lee KC, Hall DE, Hoff BA, Moffat BA, Sharma S, Chenevert TL, Meyer CR, Leopold WR, Johnson TD, Mazurchuk RV, Rehemtulla A, Ross BD. Dynamic imaging of emerging resistance during cancer therapy. Cancer Res 2006;66:4687–92. [PubMed: 16651420]
23. Mathieu V, De Nève N, Le Mercier M, Dewelle J, Gaussin JF, Dehoux M, Kiss R, Lefranc F. Combining bevacizumab with temozolomide increases the antitumor efficacy of temozolomide in a human glioblastoma orthotopic xenograft model. Neoplasia 2008;10:1383–92. [PubMed: 19048117]
24. McKeage MJ, Fong P, Jeffery M, Baguley BC, Kestell P, Ravic M, Jameson MB. 5,6-Dimethylxanthenone-4-acetic acid in the treatment of refractory tumors: a phase I safety study of a vascular disrupting agent. Clin Cancer Res 2006;12:1776–84. [PubMed: 16551862]
25. McKeage MJ, Von Pawel J, Reck M, Jameson MB, Rosenthal MA, Sullivan R, Gibbs D, Mainwaring PN, Serke M, Lafitte JJ, Chouaid C, Freitag L, Quoix E. Randomised phase II study of ASA404 combined with carboplatin and paclitaxel in previously untreated advanced non-small cell lung cancer. Br J Cancer 2008;99:2006–12. [PubMed: 19078952]
26. Narayana A, Kelly P, Golfinos J, Parker E, Johnson G, Knopp E, Zagzag D, Fischer I, Raza S, Medabalmi P, Eagan P, Gruber ML. Antiangiogenic therapy using bevacizumab in recurrent high-grade glioma: impact on local control and patient survival. J Neurosurg 2009;110:173–80. [PubMed: 18834263]
27. Raatschen HJ, Simon GH, Fu Y, Sennino B, Shames DM, Wendland MF, McDonald DM, Brasch RC. Vascular permeability during antiangiogenesis treatment: MR imaging assay results as biomarker for subsequent tumor growth in rats. Radiology 2008;247:391–9. [PubMed: 18372448]
28. Rehman F, Rustin G. ASA404: update on drug development. Expert Opin Investig Drugs 2008;17:1547–51.

29. Ruoslahti E. Specialization of tumor vasculature. Nat Rev Cancer 2002;2:83–90. [PubMed: 12635171]
30. Sandstrom M, Johansson M, Andersson U, Bergh A, Bergenheim AT, Henriksson R. The tyrosine kinase inhibitor ZD6474 inhibits tumor growth in an intracerebral rat glioma model. Br J Cancer 2004;91:1174–80. [PubMed: 15305185]
31. Schmiedl U, Brasch RC, Ogan MD, Moseley ME. Albumin labeled with Gd-DTPA. An intravascular contrast-enhancing agent for magnetic resonance blood pool and perfusion imaging. Acta Radiol suppl 1990;374:99–102. [PubMed: 1966977]
32. Seshadri M, Spernyak JA, Mazurchuk R, Camacho SH, Oseroff AR, Cheney RT, Bellnier DA. Tumor vascular response to photodynamic therapy and the antivascular agent 5,6-dimethylxanthenone-4-acetic acid: implications for combination therapy. Clin Cancer Res 2005;11:4241–50. [PubMed: 15930363]
33. Seshadri M, Mazurchuk R, Spernyak JA, Bhattacharya A, Rustum YM, Bellnier DA. Activity of the vascular disrupting agent 5,6-dimethylxanthenone-4-acetic acid against human head and neck carcinoma xenografts. Neoplasia 2006;8:534–42. [PubMed: 16867215]
34. Seshadri M, Bellnier DA, Cheney RT. Assessment of the early effects of 5,6-dimethylxanthenone-4-acetic acid using macromolecular contrast media-enhanced magnetic resonance imaging: ectopic versus orthotopic tumors. Int J Radiat Oncol Biol Phys 2008;72:1198–207. [PubMed: 18954713]
35. Sorensen AG, Batchelor TT, Wen PY, Zhang WT, Jain RK. Response criterial for glioma. Nat Clin Pract Oncol 2008;5:634–44. [PubMed: 18711427]
36. Tong R, Boucher Y, Kozin S, Winkler F, Hicklin D, Jain R. Vascular normalization by vascular endothelial growth factor receptor 2 blockade induces a pressure gradient across the vasculature and improves drug penetration in tumors. Cancer Res 2004;64:3731–6. [PubMed: 15172975]
37. Tozer GM, Kanthou C, Baguley BC. Disrupting tumour blood vessels. Nat Rev Cancer 2005;5:423–35. [PubMed: 15928673]
38. Wachsberger PR, Burd R, Marero N, Daskalakis C, Ryan A, McCue P, Dicker AP. Effect of the tumor vascular-damaging agent, ZD6126, on the radioresponse of U87 glioblastoma. Clin Cancer Res 2005;11:835–42. [PubMed: 15701874]
39. Zhao L, Ching LM, Kestell P, Kelland LR, Baguley BC. Mechanisms of tumor vascular shutdown induced by 5,6-dimethylxanthenone-4- acetic acid (DMXAA): Increased tumor vascular permeability. Int J Cancer 2005;116:322–6. [PubMed: 15800918]
40. Zuniga RM, Torcuator R, Jain R, Anderson J, Doyle T, Ellika S, Schultz L, Mikkelsen T. Efficacy, safety and patterns of response and recurrence in patients with recurrent high-grade gliomas treated with bevacizumab plus irinotecan. J Neurooncol 2009;91:329–36. [PubMed: 18953493]

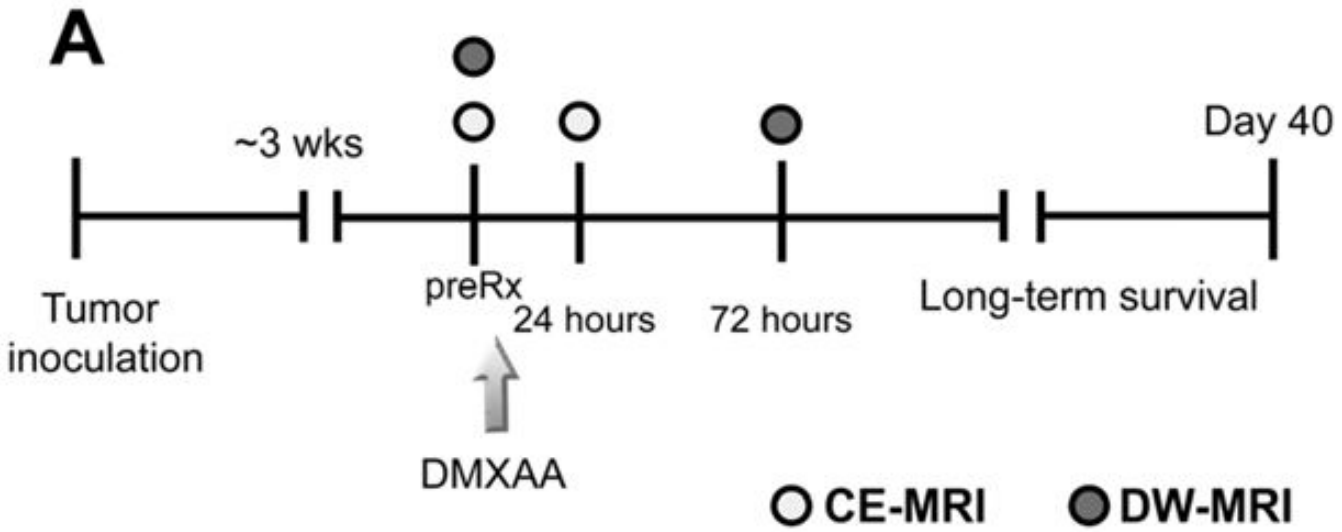

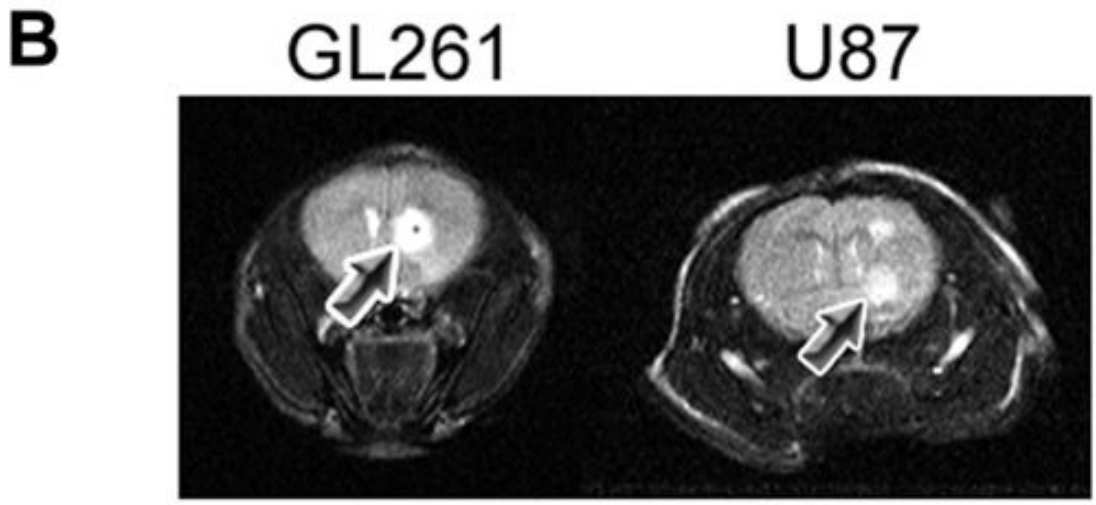

Figure 1.

(A) Schematic outline of the study design. Approximately 3 weeks post intracranial implantation of GL261 and U87 cells, tumor-bearing mice were administered a single dose of the VDA DMXAA as described in the *Materials and Methods* section. CE-MRI was performed prior to (preRx) and 24 hours following treatment to monitor the vascular response of gliomas to DMXAA treatment. Additionally, DW-MRI was performed 72 hours post treatment to examine changes in cellularity following VDA therapy. Long-term survival analysis was performed by observing animals in the control and treatment groups over a 40-day period. **(B) T2W MRI of tumor growth.** T2-weighted (T2W) MR images of a control C57Bl6 mouse bearing a GL261 glioma and a nude mouse bearing U87 glioma are shown. Tumors appeared as well-defined hyperintense regions at the site of injection as indicated by the *arrows.*

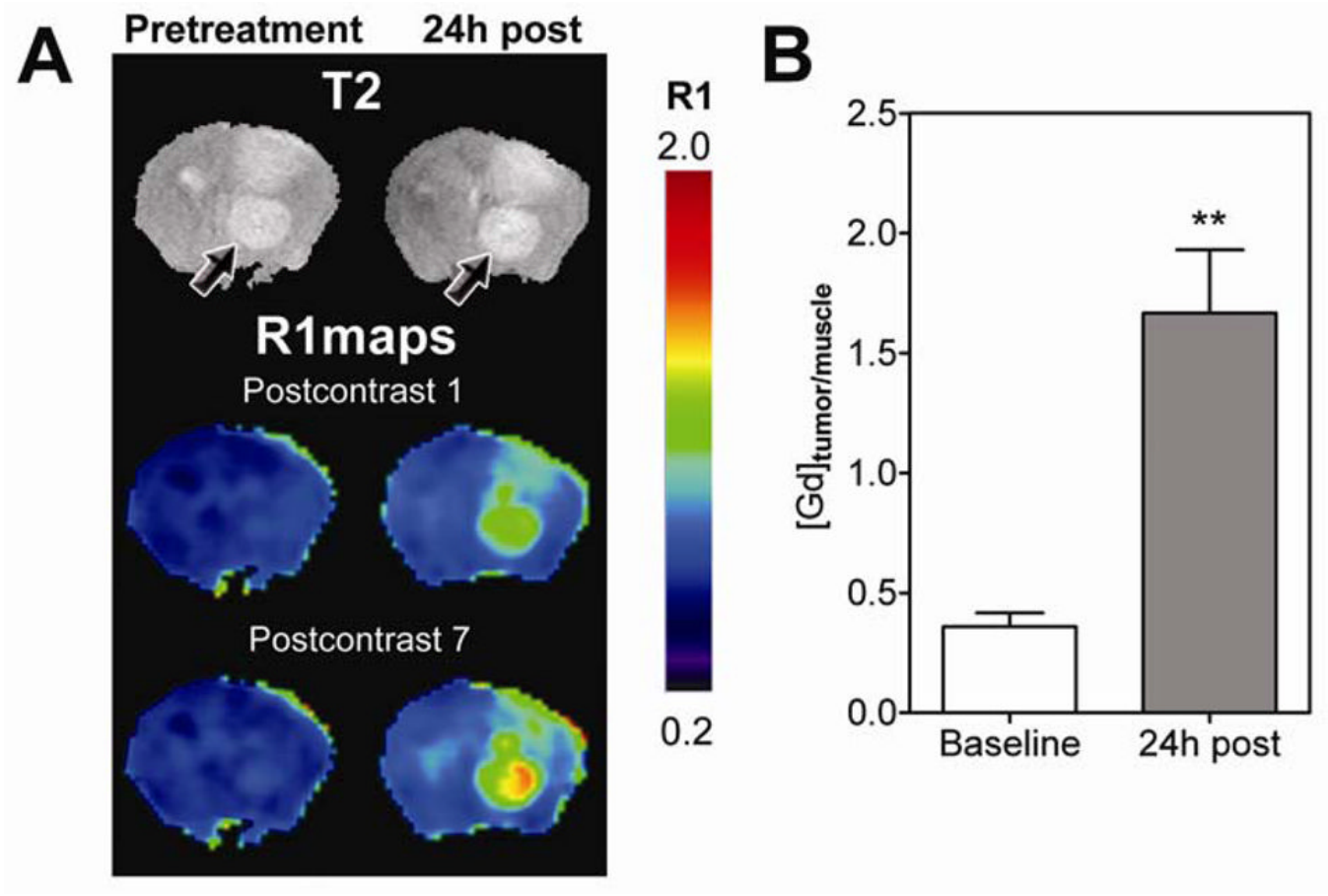

Figure 2. Contrast-enhanced MRI of Response of GL261 gliomas to VDA therapy

(A) T2W images and corresponding pseudo-colorized R1 maps of a C57Bl6 mouse brain bearing GL261 glioma before treatment and 24 hours post DMXAA treatment. R1 maps calculated from the first (1) and last (7) post contrast scans are shown at both time points. Compared to baseline images, marked extravasation of the contrast agent was observed in post contrast R1 maps indicative of tumor vascular disruption following treatment. **(B)** Bar graph represents normalized mean ΔR1 values (tumor/muscle) expressed as Gd concentration in GL261 gliomas at baseline and 24 hours post treatment. A statistically significant increase (**p<0.01) 24 hours post VDA therapy was observed compared to baseline estimates as a consequence of DMXAA-induced tumor vascular disruption.

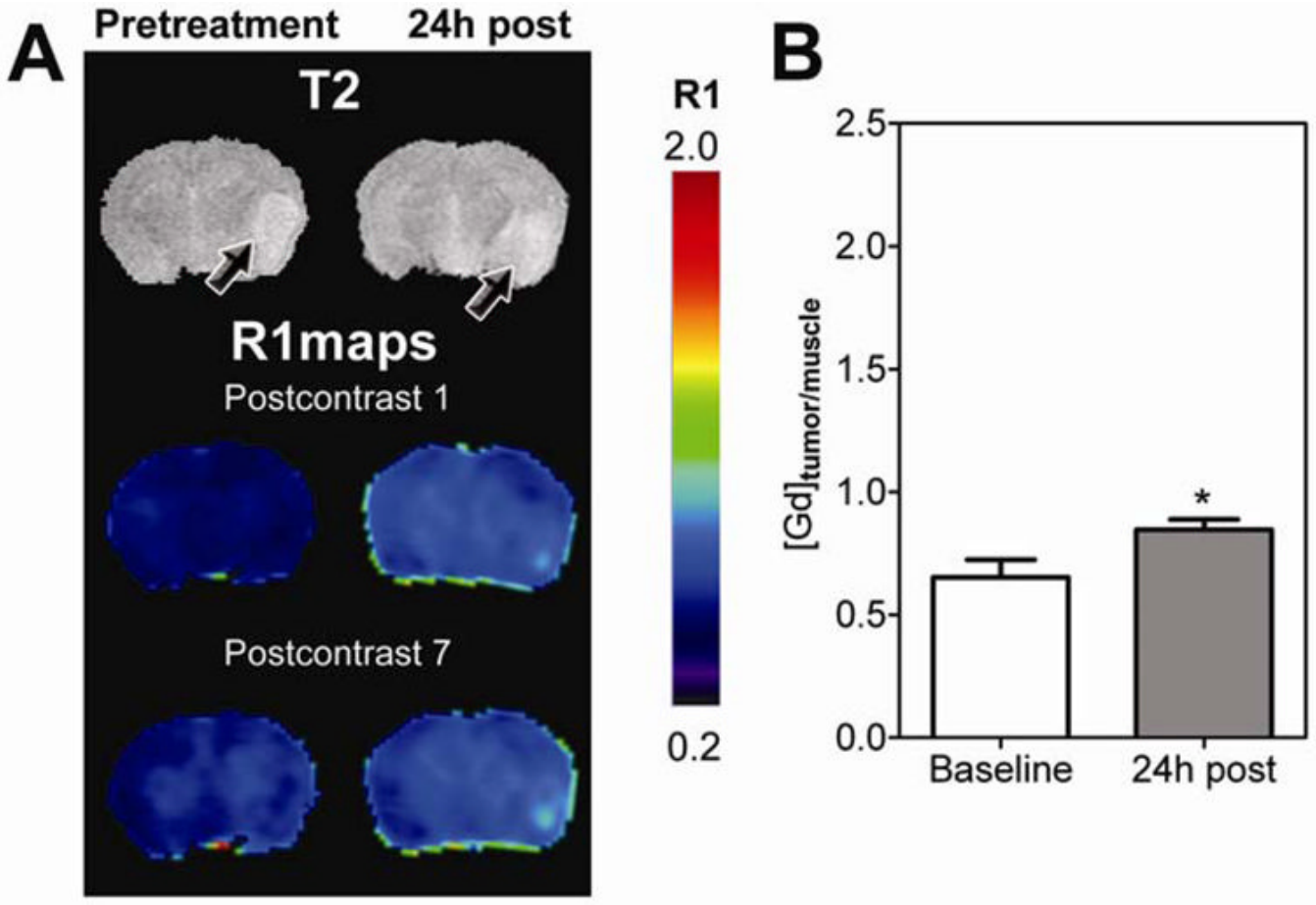

Figure 3. Vascular response of U87 gliomas to DMXAA

(A) Post contrast R1 maps of a nude mouse brain bearing U87 glioma before and after DMXAA treatment showing evidence of vascular disruption by DMXAA. R1 maps were calculated on a pixel-by-pixel basis from the first (1) and last (7) post contrast T1W scans. Corresponding T2W images are also shown. *Arrows* point to location of the tumor. **(B)** Concentration of Gd as estimated from normalized mean ΔR1 values (tumor/muscle) of U87 gliomas showing a statistically significant increase (*p<0.05) 24 hours post VDA therapy compared to baseline values.

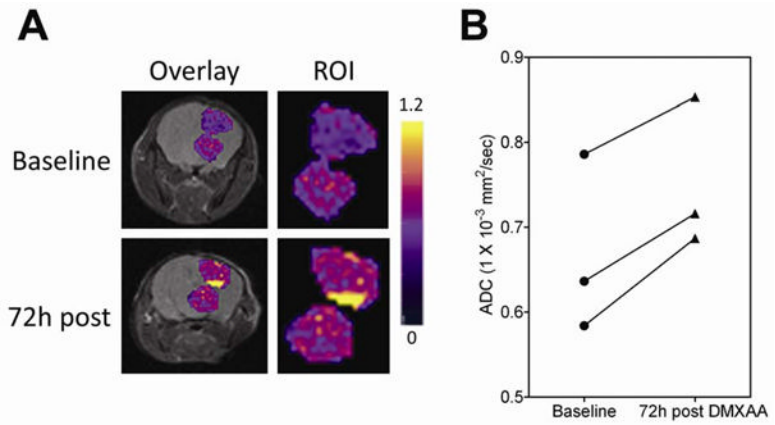

Figure 4. DW-MRI of GL261 response to DMXAA

(A) Pseudo-colorized ADC maps of a C57Bl6 mouse bearing GL261 glioma overlaid on anatomical T2W scans at baseline and 72 hours post treatment. Enlarged region of interest (ROI, tumor) is also shown. **(B)** Mean ADC values of the tumor showed a statistically significant increase at 72 hours post treatment compared to baseline values in all 3 animals (p=0.015).

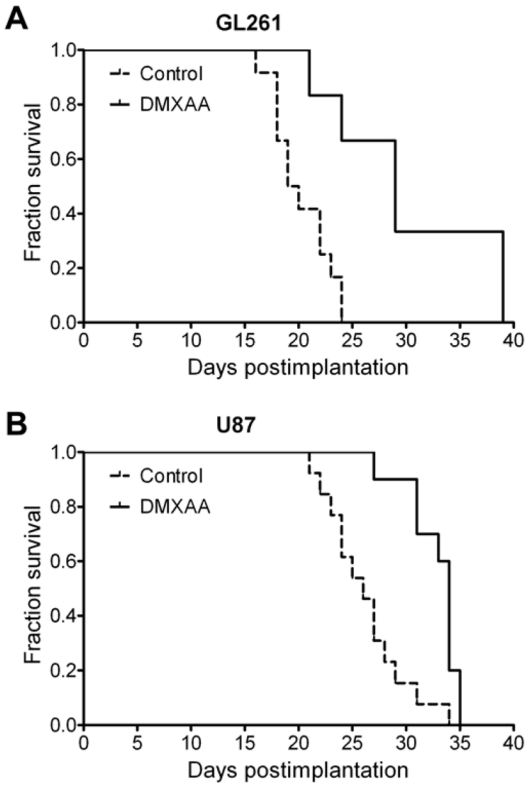

Figure 5. Therapeutic efficacy of DMXAA against gliomas

Kaplan-Meier survival analysis of GL261 **(A)** and U87 glioma-bearing animals **(B)** treated with a single dose of DMXAA (30 mg/kg – GL261; 27.5 mg/kg – U87). Differences in median survival between animals in the control and treatment groups were analyzed for statistical significance using the log-rank test. Control vs treatment groups: p=0.0028 (GL261; Controls n=12; DMXAA n=6) and p=0.0005 (U87; Controls n=13; DMXAA n=10).